Nanoscale Research Letters
a SpringerOpen Journal

NANO EXPRESS Open Access

High-performance solid-state supercapacitors based on graphene-ZnO hybrid nanocomposites

Zijiong Li[2*], Zhihua Zhou[3], Gaoqian Yun[2], Kai Shi[2], Xiaowei Lv[1] and Baocheng Yang[1*]

Abstract

In this paper, we report a facile low-cost synthesis of the graphene-ZnO hybrid nanocomposites for solid-state supercapacitors. Structural analysis revealed a homogeneous distribution of ZnO nanorods that are inserted in graphene nanosheets, forming a sandwiched architecture. The material exhibited a high specific capacitance of 156 F g^{-1} at a scan rate of 5 mV.s^{-1}. The fabricated solid-state supercapacitor device using these graphene-ZnO hybrid nanocomposites exhibits good supercapacitive performance and long-term cycle stability. The improved supercapacitance property of these materials could be ascribed to the increased conductivity of ZnO and better utilization of graphene. These results demonstrate the potential of the graphene-ZnO hybrid nanocomposites as an electrode in high-performance supercapacitors.

Keywords: Zinc oxide nanorods; Graphene nanosheets; Solid-state supercapacitor

Background

As a new class of energy storage device, supercapacitors, also known as electrochemical capacitors, has received considerable attention that can be used in hybrid electric vehicles, memory backup, and other emergency power supply devices due to their higher power density, superior cycle lifetime, and low maintenance cost. However, the energy density of supercapacitors is lower than batteries [1-6]. It is highly desirable to increase the energy density of supercapacitors to approach that of batteries, which could enable their use as primary power sources. Supercapacitors store electrical energy by two mechanisms [7,8]: electrochemical double-layer capacitance (EDLC) and pseudocapacitance. In EDLC, the capacitance comes from the charge accumulated at the electrode-electrolyte interface. Carbon-based materials are widely used in EDLC electrode due to their high surface area and excellent electric conductivity. Compared to EDLCs, pseudocapacitors can provide much higher capacitance and energy density through Faradic reaction [6,7]. Transition metal oxides and conducting polymers are the promising candidates because they can provide high energy density for pseudocapacitors. It has been found that carbon materials which combine with pseudocapacitive electrode materials can improve the capacitance of supercapacitors [8-10].

Graphene (Gr) is an atom-thick, two-dimensional (2D) material composed of a monolayer hexagonal sp^2-hybridized carbon. Gr with the maximum surface area of 2,630 m^2 g^{-1} and high intrinsic electrical conductivity is believed to be one of the most promising electrode materials for supercapacitors [11-14]. However, in practical applications, Gr nanosheets usually suffer from agglomeration or restacking due to strong van der Waals interactions [15-17], which leads to the loss of surface area and capacitance. Metal/metal oxide or metal hydroxide nanoparticles are currently introduced into the interlayer of Gr nanosheets to prevent agglomeration [18-21]. Transition metal oxides [22-25], which can contribute to pseudocapacitance such as RuO_2, have been recognized as the best electrode materials for supercapacitors. However, their expensive nature and high toxicity severely limit their practical application in a large scale. Therefore, the development of low-cost and high-abundance metal oxide as an alternative is highly desirable [26-29]. ZnO is considered to be a promising material for supercapacitors due to its high specific energy density, low cost, non-toxicity, eco-friendliness, and abundant availability.

* Correspondence: zijiongl@126.com; shimoxi2011@126.com
[2]School of Physics & Electronic Engineering, Zhengzhou University of Light Industry, Zhengzhou 450002, People's Republic of China
[1]Institute of Nano Functional Materials, Huanghe University of Science & Technology, Zhengzhou 450006, People's Republic of China
Full list of author information is available at the end of the article

Very recently, Kim et al. [30] and Pan et al. [31] reported on reduced graphene oxide-ZnO nanocomposites for supercapacitor electrodes by microwave-assisted method, which exhibited a specific capacitance of 109 F g^{-1} at a scan rate of 2 mV s^{-1} and 146 F g^{-1} at a scan rate of 2 mV s^{-1}, respectively. But only approximately 30 F g^{-1} at a scan rate of 100 mV s^{-1}. A sandwiched nanoarchitecture of reduced graphene oxide/ZnO/deducted graphene oxide is fabricated by Huang et al. [32] using chemical vapor deposition method, which exhibited a specific capacitance of 51.6 F g^{-1} at a scan rate of 10 mV s^{-1}. Additionally, graphene-ZnO nanocomposites synthesized by other method such as ultrasonic spray pyrolysis method and their electrochemical performance were reported [33,34]. However, these materials were limited by a low specific capacitance and poor stability at higher scan rate or high current densities. An effective regulation of graphene-ZnO hybrid for high performance of supercapacitors is still challenging. On the other hand, the investigation of solid-state supercapacitors based on graphene-ZnO hybrid is very limited.

In this report, a simple and facile synthesis route is developed to prepare graphene-ZnO hybrid as an electrode material for supercapacitors using one-step hydrothermal technique. Initially, graphene oxide (GO) was synthesized using the well-known modified Hummer's method. ZnO nanorods are inserted between the graphene nanosheets layer-by-layer rather than simply decorated on the surface of graphene during GO hydrothermal reduction process. This strategy provides a novel method for the preparation of highly active materials (ZnO nanorods) directly grown on Gr surface that avoids the restacking of Gr sheets, which show high specific capacitance even at higher scan rate and excellent long-term cycle stability applied in a all solid-state supercapacitor device. Such high electrochemical properties provide important prospects for graphene-ZnO hybrid to be widely used as electrode material in supercapacitor.

Methods

Materials

Graphite powder was purchased from Sigma Aldrich (St. Louis, MO, USA). All other reagents were commercially available and analytic grade and were used directly without any purification. Double-distilled water was used throughout the experiments.

Synthesis of graphene oxide

Graphite oxide was prepared from natural graphite powder through a modified Hummers method [35]. One gram of graphite powder, 1.1 g sodium nitrate, and 46 ml sulfuric acid were mixed and stirred for 10 min. Then, 3.0 g potassium permanganate was added slowly and temperature maintained below 20°C. DI water was added slowly and the temperature was raised to 90°C. The solution turned bright yellow when 3.0 ml of hydrogen peroxide (30%) was added. The mixture was filtered while warm and washed with warm DI water. Then GO was subjected to dialysis to completely remove metal ions and acids. Finally, the product was dried in air at room temperature.

Synthesis of ZnO nanorods

Pure ZnO nanorods were synthesized by hydrothermal method. In a typical experiment, 100 mg of $Zn(NO_3)_2$ was first dispersed into 30 ml deionized water. Then, 15 μl of hydrazine hydrate was added drop by drop under stirring, followed by ultrasonication for 30 min. Then the solution was transferred to a 50 ml of Teflon-lined autoclave and heated at 160°C for 12 h. Finally, the ZnO nanostructures were collected after washing and centrifugation.

Synthesis of the graphene-ZnO hybrid nanostructure

As-synthesized GO (50 mg) was dispersed in 100 ml double-distilled water; the dispersion was brown in color. The dispersed GO was exfoliated, using sonication for 1 h, and then 20 mg $Zn(NO_3)_2$ and 10 μl hydrazine hydrate were added into the abovementioned solution under ultrasonication. After hydrothermal reaction at 160°C for 12 h, the graphene-ZnO nanocomposites were synthesized and collected through washing, centrifugation, and drying.

Characterizations

The microstructure morphologies and crystal structures of the as-synthesized pure ZnO, pristine graphene, and graphene-ZnO nanocomposites were characterized using field-emission scanning electron microscope (FESEM, Quanta 250 FEG; FEI, Hillsboro, OR, USA), X-ray diffraction (XRD, D8 ADVANCE, Bruker, Billerica, MA, USA) with Cu-Kα radiation (λ = 0.154178 nm), transmission electron microscopy (TEM) (JEM2010-HR, JEOL, Akishima, Tokyo, Japan), and laser micro-Raman spectrometry (Renishaw inVia, Gloucestershire, UK). Energy dispersive spectrometer (EDS) mapping analysis was used to analyze the element distribution of the as-synthesized nanocomposites. Inductively coupled plasma atomic emission spectroscopy (ICP, SPECTRO, Birmingham, UK) was used to analyze the loading of ZnO on graphene. The electrochemical measurements were carried out on a CHI 660D electrochemical workstation (Chenhua, Shanghai, China) at room temperature.

Preparation of electrodes and electrochemical characterization

The working electrode was prepared as follows: approximately 10 mg of as-synthesized material was first mixed with polytetrafluoroethylene (60 wt.% water suspension;

Sigma-Aldrich, St. Louis, MO, USA) in a ratio of 100:1 by weight and then dispersed in ethanol. The suspension was drop-dried into a 1 cm × 1 cm Ni foam (2-mm thick) at 80°C. The sample loaded foam was compressed before measurement.

The electrochemical measurements including cyclic voltammograms (CVs), galvanostatic charge/discharge, and electrochemical impedance spectroscopy were performed in a three-electrode setup: a Ni foam coated with the active materials serving as the working electrode, a platinum foil electrode, and a saturated calomel electrode (SCE) serving as the counter and reference electrodes, respectively.

Fabrication of solid-state supercapacitors

The device was assembled by two pieces of graphene-ZnO electrodes with a separator (Whatman 8-μm filter paper) sandwiched in between and polyvinyl alcohol (PVA)-gelled as a solid electrolyte. The PVA-gel electrolyte was made by following method. 600 mg PVA was mixed with 5 ml Milli-Q water (Millipore Corp., Billerica, MA, USA). The mixture was heated at 80°C under stirring for 30 min and then cooled naturally. Then approximately 10 ml of 0.5 M $NaNO_3$ was added to the mixture and stirred for 30 min. The graphene-ZnO hybrid materials were collected on a Teflon membrane (0.2-m pore size) by vacuum filtration and then pressed onto the carbon-coated Al current collector. The graphene-ZnO electrodes and a separator were sandwiched together in a stainless steel cell for the fully assembled two-electrode cell device.

Results and discussion

Figure 1 shows the typical images of pristine GO, ZnO, and the as-synthesized graphene-ZnO nanocomposites. Figure 1a presents SEM images of the GO film, showing a stack of layered laminas composed of complex fold and pockets of void space. It is conspicuous to observe the edges of individual sheets, including the crumpled and continuous areas. The ZnO nanorods with smooth surface and high crystallinity can be observed from Figure 1b. The diameters of ZnO nanorods are typically in the range of approximately 20 to 30 nm. After ZnO was inserted in GO sheets by hydrothermal method, typical SEM images were taken and are shown in Figure 1c,d. It is found that the ZnO nanorods are dispersed uniformly on the surface of Gr. The ZnO nanorods were sandwiched in between Gr layers so that Gr sheets are loosely stacked into continuous films without apparent stacking order.

The TEM image (Figure 2a) identifies that the ZnO nanorods with an average diameter of approximately 20 nm are dispersed into the Gr layers. The uniform distribution of ZnO nanorods among the Gr is due to the *in situ* hydrothermal reduction on the surface of Gr. The high-resolution TEM (HRTEM) and the selected-area electron diffraction (SAED) pattern of the graphene-ZnO hybrid nanostructure (Figure 2b) confirmed the hexagonal wurtzite phase of ZnO nanorods.

Figure 3a shows the typical XRD patterns of ZnO and the as-synthesized graphene-ZnO hybrid nanostructure. It is found that the XRD pattern of ZnO consists of five diffraction peaks at 32.6°, 35°, 36.8°, 47.8°, 56.5°, 62.5°, and 67.6°, corresponding to the (100), (002), (101), (102), (110), (103), and (112) planes of the hexagonal wurtzite ZnO phase (JCPDS 65–3411), respectively. From the XRD pattern of the graphene-ZnO hybrid nanostructure, a strong and broad peak appeared at a 2θ value of 25°, which corresponded to the (002) plane of Gr . No other peaks of GO observed indicate that GO is completely reduced to a Gr sheet. Other peaks observed in the XRD pattern matched the hexagonal wurtzite ZnO, indicating a well hybrid. The EDS spectrum of the graphene-ZnO hybrid nanostructure is shown in Figure 3b. The spectrum clearly showed the presence of carbon (C), zinc (Zn), and oxygen (O) elements in the graphene-ZnO hybrid nanostructure. The Zn and O elements originated from the ZnO nanorods, and the C was contributed by the Gr nanosheets. Thermogravimetric analysis (TGA) of Sn-Gr composite was performed to find out metal oxide content in the sample. Figure 3c shows the TGA profiles of GO and graphene-ZnO hybrid nanostructure measured in air conditions. After the product had been calcined at 900°C in air, the residue of GO is approximately 5 wt.%, while the graphene-ZnO hybrid sample is approximately 38.5 wt.%. Therefore, the ZnO content in the graphene-ZnO sample was determined to be about 33.5 wt.%. In addition, the lower thermal stability of the graphene-ZnO compared to the pristine GO may be due to the catalytic decomposition of ZnO since carbon has been reported to catalytically decompose oxides. To further confirm the formation of the samples, Raman detection was performed. Figure 3d shows the Raman spectra of graphene-ZnO hybrid nanostructure. A very intense Raman band can be seen at 1,354 and 1,596 cm^{-1}, which corresponded to the well-documented D and G bands, respectively. The D band is a common feature for sp^3 defects or disorder in carbon, and the G band provides useful information on in-plane vibrations of sp^2-bonded carbon atoms in a 2D hexagonal lattice. The 2D band appeared in the sample, indicating the conversion of GO into Gr sheets. Further observation showed that three vibrational peaks at 323, 437, and 487 cm^{-1} were also observed (inset in Figure 3d), which correspond to the to the optical phonon E_2 mode of wurtzite hexagonal phase of ZnO.

To study the electrochemical performance of the graphene-ZnO hybrid nanostructure, electrochemical measurements were conducted in a three-electrode electrochemical cell with a Pt wire as counter electrode and a SCE as reference electrode in 0.5 M Na_2SO_4 solution. In

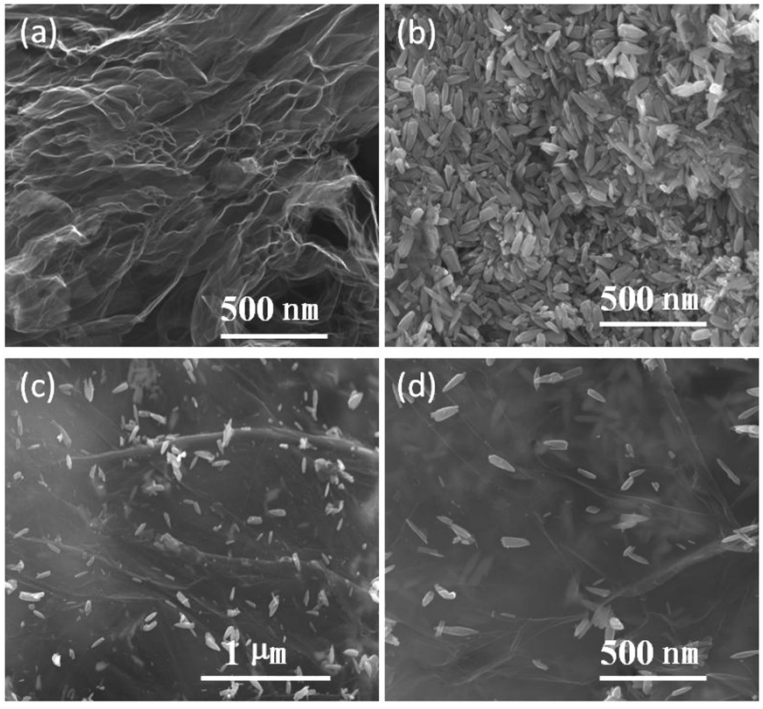

Figure 1 SEM images. GO **(a)**, ZnO **(b)**, low and high magnification of graphene-ZnO hybrid nanostructure **(c, d)**.

order to illustrate the advantage of the graphene-ZnO hybrid nanostructure, Figure 4a compares the cyclic voltammetry (CV) curves of pristine Gr sheets, ZnO nanorods, and graphene-ZnO hybrid nanostructure at 5 mV s^{-1}. It can be seen that all these curves exhibit nearly rectangular shape, indicating ideal supercapacitive behavior. In comparison to the ZnO nanorods and pristine Gr electrodes, the graphene-ZnO hybrid nanostructure electrode showed a higher integrated area, which reveals the superior electrochemical performance of the graphene-ZnO hybrid electrode. The specific capacitance (C_s) values were calculated from the CV curves using the following equation [36]:

$$C_s = \frac{\int I(u)\mathrm{d}t}{m \times v \times \Delta V} \quad (1)$$

where I is the oxidation or reduction current, dt is time differential, m indicates the mass of the active electrode material, and ΔV indicates the voltage range of one sweep segment. According to Equation 1, the calculated C_s values of ZnO nanorods, pristine Gr sheets, and the

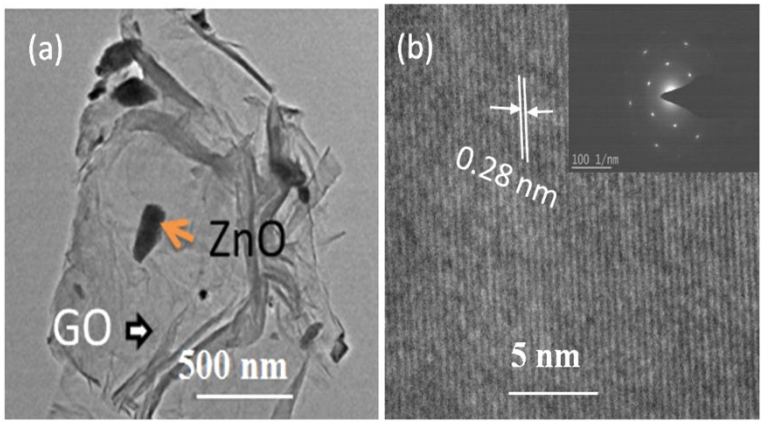

Figure 2 TEM image (a) and HRTEM image (b) of graphene-ZnO nanocomposites. Inset of **(b)** is the corresponding SAED pattern.

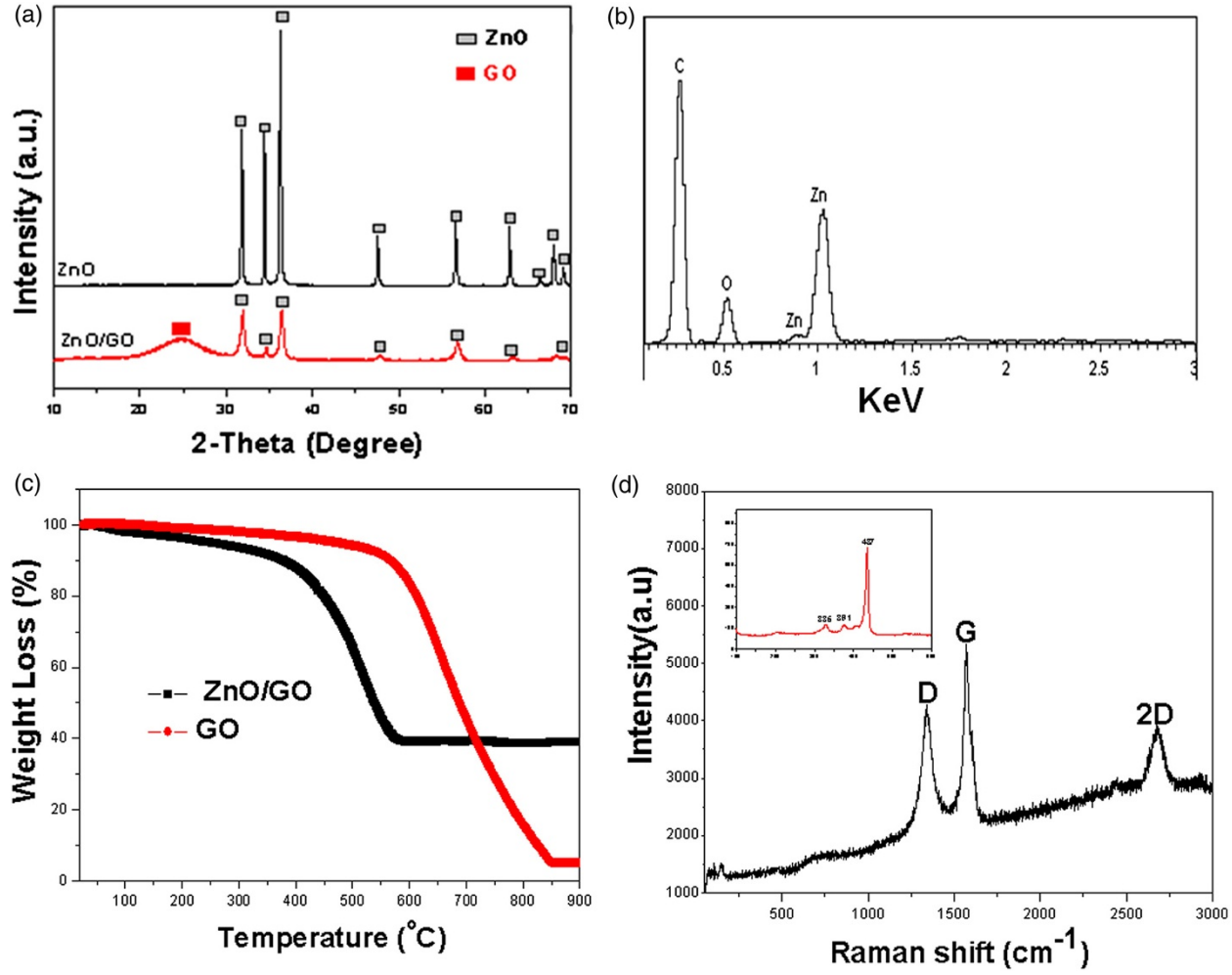

Figure 3 Characterization of ZnO, graphene-ZnO, graphene-ZnO hybrid nanostructures. (a) XRD patterns of ZnO and graphene-ZnO. **(b)** EDS image of the graphene-ZnO hybrid nanostructure. **(c)** TGA curves of GO and graphene-ZnO sample, heating rate 10°C min^{-1}. **(d)** Raman spectra of graphene-ZnO hybrid nanostructure.

graphene-ZnO hybrid electrode are 36, 112, and 156 F g^{-1}, respectively, at a scan rate of 5 mV s^{-1}. The specific capacitance of the graphene-ZnO hybrid electrode was much higher than that of the ZnO nanorods and pristine Gr sheets. Moreover, this value is higher than that of previously reported. To obtain a more detailed information on the capacitance performance of the as-prepared graphene-ZnO hybrid nanostructure, the CV curves with various scan rates were studied. Figure 4b summed the C_s of ZnO, pristine Gr, and graphene-ZnO hybrid electrodes at various scan rates. It can be seen that the specific capacitance decreased with an increase in the scan rate from 5 to 500 mV s^{-1}. The reason may be that insufficient time available for ion diffusion and adsorption inside the smallest pores within a large particle at high scan rates [37]. Moreover, the C_s of the graphene-ZnO hybrid electrode was much higher than that of a ZnO and pristine Gr electrodes for all the scan rates tested. Figure 4c shows galvanostatic charge–discharge measurements of the graphene-ZnO hybrid electrode at a constant current density of 2.0 mA cm^{-2}. It can be seen that the curves were linear and exhibited a typical triangular shape even charging/discharging for 12,000 s, which indicated good electrochemical capacitive characteristics. The enhanced electrochemical performance of the graphene-ZnO hybrid can be attributed to the sandwiched structure. Here, the graphene in the hybrid electrode provides better electronic conductivity and excellent interfacial contact between ZnO and graphene, which results in the fast transportation of electrons throughout the entire electrode matrix [38]. Moreover, it is evident that when the ZnO size is reduced to nanometer dimensions, the surface area and electroactive sites increase, which effectively reduces the diffusion length of the Na^+ ion in the electrode matrix [39,40].

Electrochemical impedance spectroscopy (EIS) was conducted to understand the conductivity, mechanistic

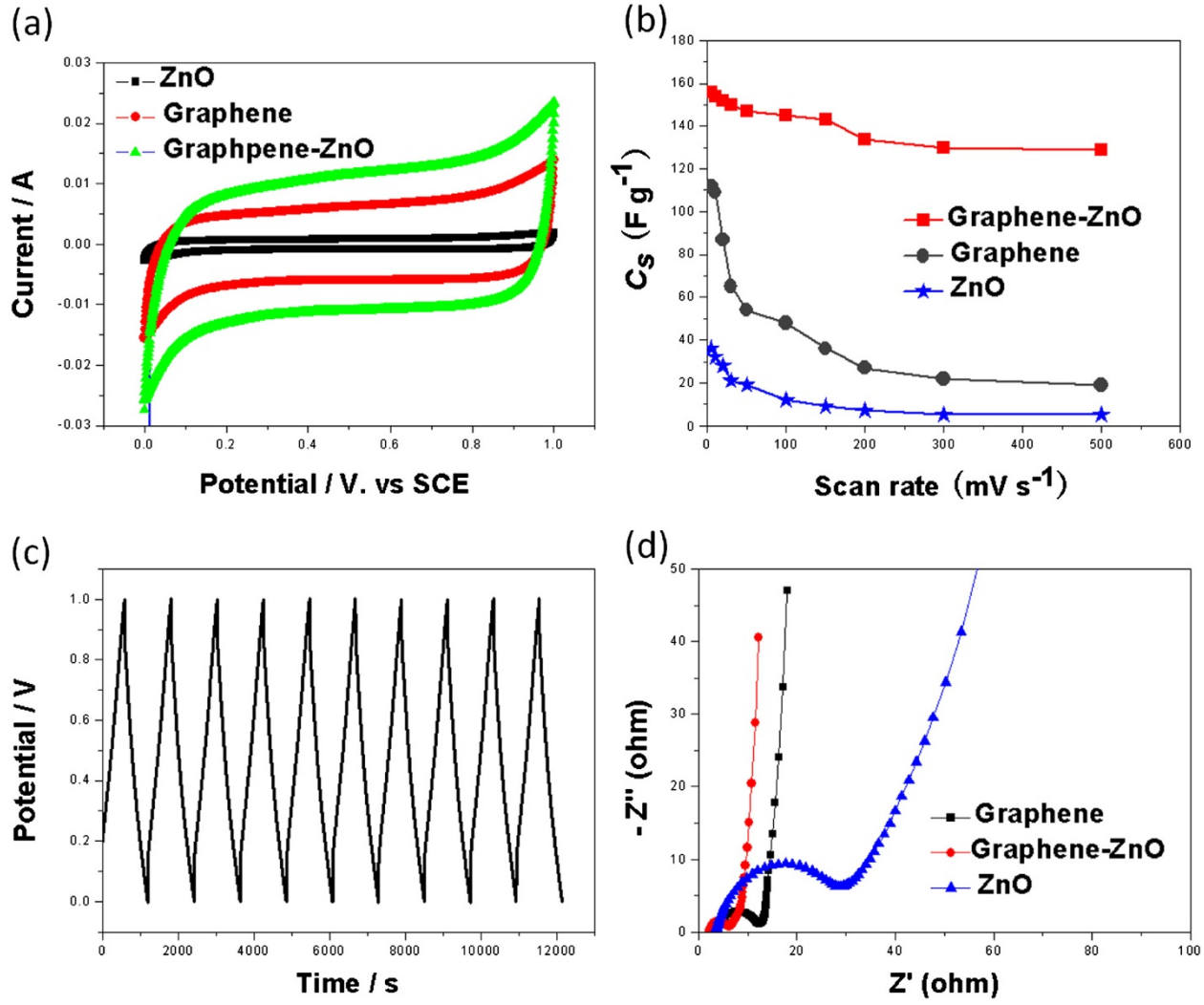

Figure 4 CV curves, specific capacitance, galvanostatic charge–discharge curve, and Nyquist plots of electrodes. (a) CV curves of the as-prepared ZnO, graphene and the graphene-ZnO hybrid electrode at a scan rate of 5 mV s^{-1} in 0.5 M Na_2SO_4 electrolyte solution. **(b)** Specific capacitance of ZnO, pristine graphene, and the graphene-ZnO hybrid electrode at different scan rates calculated from CV curves. **(c)** Galvanostatic charge–discharge curve of the graphene-ZnO hybrid electrode at a constant current density of 2.0 mA cm^{-2}. **(d)** Nyquist plots for ZnO, pristine graphene, and the graphene-ZnO hybrid electrode.

analysis of interfacial processes and structure, and charge transport in the material/electrolyte interface of these electrodes. Figure 4d shows the Nyquist plots for the ZnO, pristine Gr, and graphene-ZnO hybrid electrodes. All these plots display a semicircle in the high-frequency region and a straight line in the low-frequency region. The straight line in the low-frequency range is called the Warburg resistance, which is caused by the frequency dependence of ion diffusion/transport from the electrolyte to the electrode surfaces [41]. The arc for the very high-frequency range corresponded to the charge transfer limiting process and was ascribed to the double-layer capacitance in parallel with the charge transfer resistance (Rct) at the contact interface between the electrode and electrolyte solution [42]. The Rct can be directly measured from the Nyquist plots as the semicircular arc diameter. The Rct for the graphene-ZnO hybrid electrode is 3.5 Ω, which is substantially smaller than those of pristine ZnO (26.4 Ω) and Gr (8.2 Ω) electrodes, indicating the better conductivity of the graphene-ZnO hybrid electrode. It indicated the incorporation of ZnO nanorods into the graphene nanosheets, resulting in an improved charge transfer performance for the electrode. Figure 5 showed the effects of ZnO amount on electrochemical properties. It can be seen that increasing the ZnO content can improve the electrochemical properties of graphene-ZnO hybrid. However, the electrochemical properties of graphene-ZnO hybrid decreased when the ZnO content is

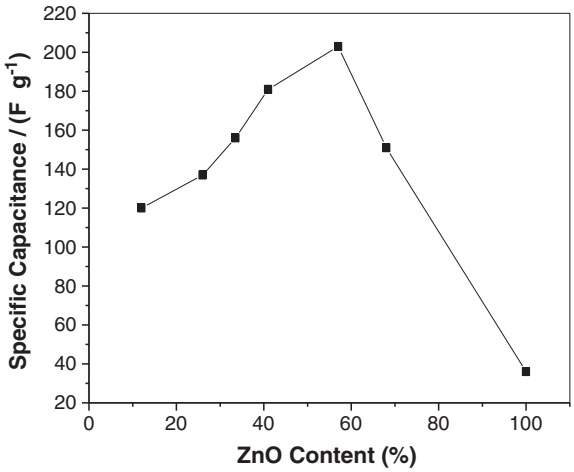

Figure 5 Effects of ZnO amount on electrochemical properties.

excess 60%. The reason is due to the poor conductivity of ZnO.

To test their feasibility for application as an energy storage device, solid-state symmetrical supercapacitors based on graphene-ZnO hybrid were fabricated by sandwiching H_2SO_4-PVA-based solid-state electrolyte between two pieces of graphene-ZnO electrodes (Figure 6a). CV curves of the solid-state supercapacitor device measured at various scan rates are collected in Figure 6b. All the CV curves exhibit a rectangular-like shape, which reveals the ideal capacitive behavior and fast charge–discharge behavior. Figure 6c shows the galvanostatic charge–discharge curves of the solid-state supercapacitor device collected at different current densities. The discharge curves of this device are relatively symmetrical with its corresponding charge counterparts, confirming the good capacitive behavior and fast charge–discharge behavior of the fabricated

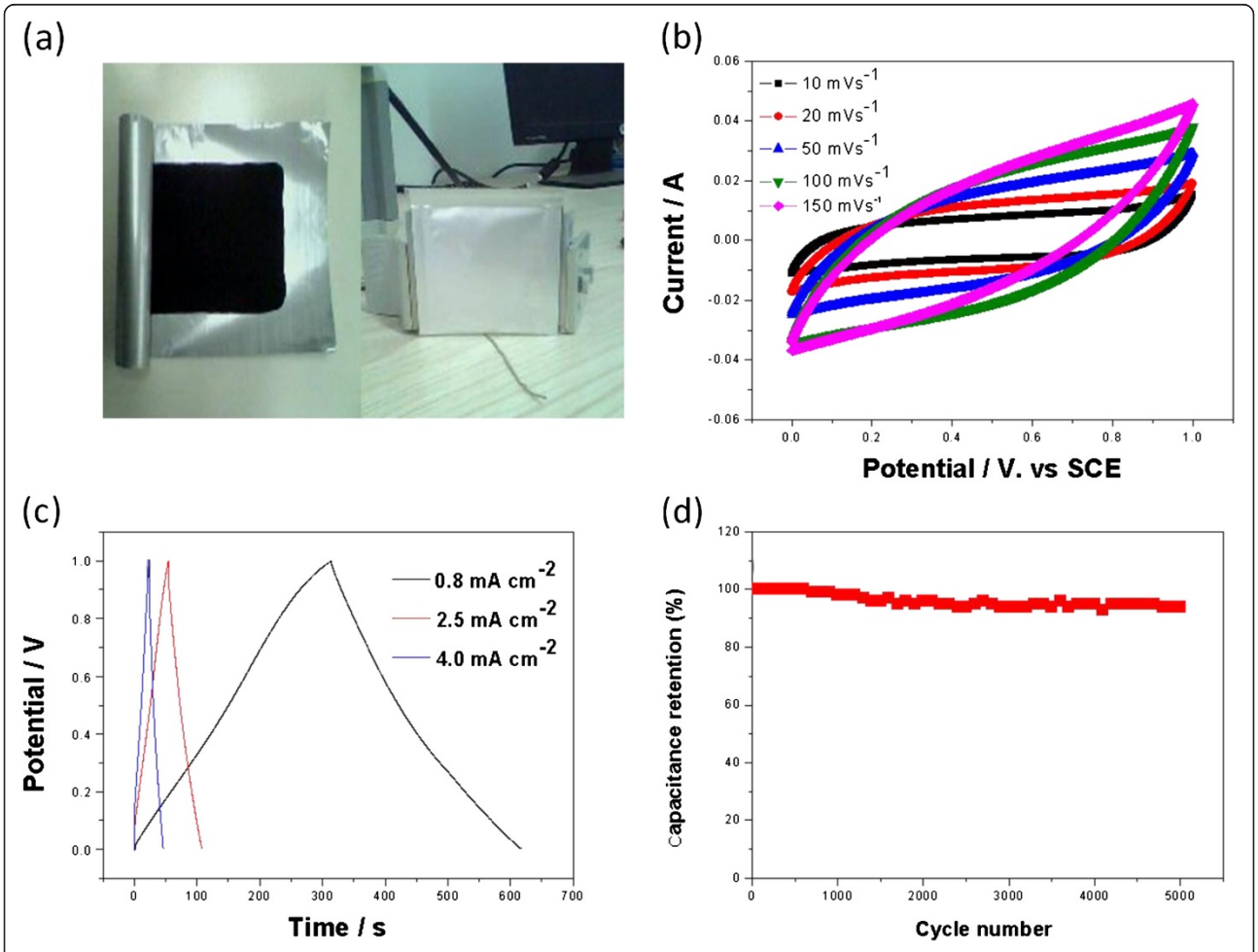

Figure 6 Supercapacitance properties of graphene-ZnO hybrid in all-solid supercapacitors. (a) Fabricated solid-state supercapacitor device-based graphene-ZnO hybrid electrode. **(b)** CV curves of the graphene-ZnO hybrid electrode at different scan rates from 10 to 150 mV s^{-1}. **(c)** Galvanostatic charge–discharge curves of the graphene-ZnO hybrid electrode at different current densities. **(d)** Variation of the specific capacitance of the graphene-ZnO hybrid electrode as a function of cycle number.

supercapacitor device. The specific capacitance for the electrodes can be obtained from charge–discharge data according to Equation 2

$$C = \frac{I \times \Delta t}{m \times \Delta V} \quad (2)$$

where C (F g^{-1}) is the specific capacitance, I (A) is the constant discharging current, Δt (s) is the discharging time, ΔV (V) is the potential window, and m (g) is the mass loading of the active material in the working. The specific capacitances of the graphene-ZnO hybrid electrode are 196, 115, and 102 F g^{-1} at the current densities of 0.8, 2.5, and 4.0 mA cm^{-2}, respectively. Additionally, the specific capacitance values decreased with increasing current density. However, the present values are higher than the previously reported even at high current density. The average energy density (E) and power density (P) were derived from the CV curves at different scan rates using the following equations [43]:

$$E = \frac{0.5 \times C(\Delta V)^2}{3.6} \quad (3)$$

$$P = \frac{E \times 3,600}{\Delta t} \quad (4)$$

where E is the average energy density of the electrode (W h kg^{-1}), P is the average power density (W kg^{-1}), C is the specific capacitance of the active material (F g^{-1}), ΔV is the voltage range of one sweep segment, and Δt (s) is the time for a sweep segment. The calculated average energy density and power density of the graphene-ZnO hybrid electrode were approximately 21.7 W h kg^{-1} and 2.6 kW kg^{-1}, respectively, at a scan rate of 5 mV s^{-1}.

The long cycle life of the supercapacitors is an important parameter for their practical application. The cycle stability of the graphene-ZnO hybrid electrode was further evaluated by repeating the CV measurements between 0 and 1.0 V at a scan rate of 100 mV s^{-1} for 5,000 cycles. Figure 6d shows the capacitance retention ratio as a function of cycle number. The capacitance of graphene-ZnO hybrid electrode retained 94% of its initial capacitor after 5,000 cycles (Figure 6d), which demonstrates excellent electrochemical stability. From these results, we concluded that the graphene-ZnO hybrid electrode materials showed a higher specific capacitance, significantly improved energy density, and excellent cycling performance.

The better electrochemical performance of the as-prepared graphene-ZnO electrode can be attributed to the following aspects: On the one hand, Gr sheets in the hybrid structure can act as a conducting agent, which greatly improves the electrical conductivity of the hybrid structure. On the other hand, the small size of the ZnO nanorods uniformly dispersed between the Gr sheets can effectively prevent the agglomeration and restacking of the Gr nanosheets, resulting in an EDLC for the overall specific capacitance. At the same time, Gr nanosheet with a large surface area in the hybrid structure not only provided double-layer capacitance to the overall energy storage but also effectively inhibited the aggregation of ZnO nanorods, resulting in fast electron transfer throughout the entire electrode matrix as well as an overall improvement in the electrochemical performance. Moreover, the nanometer-sized smaller ZnO rods facilitate faster charge–discharge rates, because the faradaic reaction replaced the diffusion-controlled Na^+ ion intercalation process which usually occurs at the ZnO surface [44]. Therefore, the supercapacitive performance of graphene-ZnO hybrid based supercapacitor is significant improved.

Conclusions

In summary, the graphene-ZnO hybrid nanostructure as an electrode material for solid-state supercapacitors was successfully synthesized using one-step hydrothermal method. The surface morphology, microstructure, composition, and capacitive behaviors of the as-prepared materials were well investigated. SEM and TEM images revealed the uniform distribution of ZnO nanorods on the Gr sheet substrate. In comparison with the specific capacitance of ZnO and pristine Gr electrode, the specific capacitance of graphene-ZnO hybrid electrode (156 F g^{-1} at a scan rate of 5 mV s^{-1}) is significantly improved. Moreover, the material exhibited excellent electrochemical stability. The improved supercapacitance performance of the graphene-ZnO hybrid was mainly attributed to the pseudocapacitance of the ZnO phase and the intrinsic double-layer capacitance of the Gr sheets. The low price, abundant resources, and environmental friendliness of ZnO may render their nanocomposites a promising candidate for practical applications.

Competing interests

The authors declare that they have no competing interests.

Authors' contributions

ZL carried out the experiment and drafted the manuscript. ZZ and XL performed the statistical analysis. GY and KS conceived of the study. BY participated in its design and coordination. All authors read and approved the final manuscript.

Acknowledgements

The authors are grateful for support from the National Natural Science and Henan Province United Foundation of China (no. U1204601 and no. 51072063), Natural Science Foundation of Henan Province (no. 122300410298), Natural Science Foundation of Education Department of Henan Province (no. 13A480365), and PhD Foundation of Zhengzhou University of Light Industry (no. 2010 BSJJ 029).

Author details

[1]Institute of Nano Functional Materials, Huanghe University of Science & Technology, Zhengzhou 450006, People's Republic of China. [2]School of Physics & Electronic Engineering, Zhengzhou University of Light Industry, Zhengzhou 450002, People's Republic of China. [3]School of Microelectronics and Solid-State Electronics, University of Electronic Science and Technology of China, Chengdu 610054, People's Republic of China.

Received: 17 September 2013 Accepted: 31 October 2013
Published: 12 November 2013

References

1. Yuan LY, Xiao X, Ding TP, Zhong JW, Zhang XH, Shen Y, Hu B, Huang YH, Zhou J, Wang ZL: **Paper-based supercapacitors for self-powered nanosystems.** *Angew Chem Int Ed* 2012, **51:**4934–4938.
2. Li ZJ, Zhou YJ, Zhang YF: **Semiconducting single-walled carbon nanotubes synthesized by S-doping.** *Nano-Micro Lett* 2009, **1:**9–13.
3. Zhai T, Wang FX, Yu MH, Xie SL, Liang CL, Li C, Xiao FM, Tang RH, Wu QX, Lu XH, Tong YX: **3D MnO2–graphene composites with large areal capacitance for high-performance asymmetric supercapacitors.** *Nanoscale* 2013, **5:**6790–6796.
4. Wu J, Wang ZM, Dorogan VG, Li SB, Zhou ZH, Li HD, Lee JH, Kim ES, Mazur YI, Salamo GJ: **Experimental analysis of the quasi-Fermi level split in quantum dot intermediate-band solar cells.** *Appl Phys Lett* 2012, **101:**043904.
5. Chang TQ, Li ZJ, Yun GQ, Jia Y, Yang HJ: **Enhanced photocatalytic activity of ZnO/CuO nanocomposites synthesized by hydrothermal method.** *Nano-Micro Lett* 2013, **5**(3):163–168.
6. Yuan LY, Lu XH, Xiao X, Zhai T, Dai JJ, Zhang FC, Hu B, Wang X, Gong L, Chen J, Hu CG, Tong YX, Zhou J, Wang ZL: **Supercapacitors based on carbon nanoparticles/MnO2. nanorods hybrid structure.** *ACS Nano* 2012, **6:**656–661.
7. Lu XH, Zheng DZ, Zhai T, Liu ZQ, Huang YY, Xie SL, Tong YX: **Large-area manganese oxide nanorod arrays as high-performance electrochemical supercapacitor.** *Energy Environ Sci* 2011, **4:**2915–2921.
8. Zhang JT, Jiang JW, Li HL, Zhao XS: **Supercapacitor fabricated with graphene-based electrodes.** *Energy Environ Sci* 2011, **4:**4009–4015.
9. El-Kady MF, Strong V, Dubin S, Kaner RB: **Laser scribing of high-performance and flexible graphene-based electrochemical capacitors.** *Science* 2012, **335:**1326–1330.
10. Liu C, Li F, Ma LP, Cheng HM: **Advanced materials for energy storage.** *Adv Mater* 2010, **22:**E28–E62.
11. Christen T, Carlen MW: **Theory of ragone plots.** *J Power Sources* 2000, **91:**210–216.
12. Hu LB, Choi JW, Yang Y, Jeong S, La Mantia F, Cui LF, Cui Y: **Beyond batteries: storing power in a sheet of paper.** *Proc Natl Acad Sci USA* 2009, **106:**21490–21494.
13. Zheng HM, Zhai T, Yu MH, Xie SL, Liang CL, Zhao WX, Wang SC, Zhang ZS, Lu XH: **TiO2@C core-shell nanowires for high-performance and flexible solid-state supercapacitors.** *J Mater Chem C* 2013, **1:**225–229.
14. Liu YZ, Li YF, Yang YG, Wen YF, Wang MZ: **A one-pot method for producing ZnO-graphene nanocomposites from graphene oxide for supercapacitors.** *Scripta Materials* 2013, **68**(5):301–304.
15. Lu XH, Wang GM, Zhai T, Yu MH, Gan JY, Tong YX, Li Y: **Hydrogenated TiO_2 nanotube arrays for supercapacitors.** *Nano Lett* 2012, **12:**1690–1696.
16. Meng FH, Ding Y: **Sub-micrometer-thick all-solid-state. supercapacitors with high power and energy densities.** *Adv Mater* 2011, **23:**4098–4102.
17. Choi BG, Chang SJ, Kang HW, Park CP, Kim HJ, Hong WH, Lee S, Huh YS: **Flexible asymmetric supercapacitor based on graphene films.** *Nanoscale* 2012, **4:**4983–4988.
18. Yu HJ, Wu JH, Fan LQ, Lin YZ, Xu KQ, Tang ZY, Cheng CX, Tang S, Lin JM, Huang ML, Lan Z: **A new strategy to enhance low-temperature capacitance: combination of two charge-storage mechanisms.** *J Power Sources* 2012, **198:**402–407.
19. Yao CZ, Wei BH, Meng LX, Li H, Gong QJ, Sun H, Ma HX, Hu XH: **Controllable electrochemical synthesis and photovoltaic performance of ZnO/CdS core-shell nanorod arrays on fluorine-doped tin oxide.** *J Power Sources* 2012, **207:**222–228.
20. Lu T, Zhang Y, Li H, Pan L, Li Y, Sun Z: **Electrochemical behaviors of graphene-ZnO and graphene-SnO_2 composite films for supercapacitors.** *Electrochmica Acta* 2010, **55:**4170–4173.
21. Yuan DS, Zhou TX, Zhou SL, Zou WJ, Mo SS, Xia NN: **Nitrogen-enriched carbon nanowires from the direct carbonization of polyaniline nanowires and its electrochemical properties.** *Electrochem Commun* 2011, **13:**242–246.
22. William YS, Hummers JR, Offeman RE: **Preparation of graphitic oxide.** *J Am Chem Soc* 1958, **80:**1339–1339.
23. Yoo EJ, Kim J, Hosono E, Zhou HS, Kudo T, Honma I: **Large reversible Li storage of grapheme nanosheet families for use in rechargeable lithium ion batteries.** *Nano Lett* 2008, **8:**2277–2282.
24. Kim BJ, Jang H, Lee SK, Hong BH, Ahn JH, Cho JH: **High-performance flexible graphene field effect transistors with ion gel gate dielectrics.** *Nano Lett* 2010, **10:**3464–3466.
25. Marcinek M, Hardwick LJ, Richardson TJ, Song X, Kostecki RJ: **Microwave plasma chemical vapor deposition of nano-structured Sn/C composite thin-film anodes for Li-ion batteries.** *J Power Sources* 2007, **173:**965–971.
26. Wang GM, Wang HY, Ling YC, Tang YC, Yang XY, Fitzmorris RC, Wang CC, Zhang JZ, Li Y: **Hydrogen-treated TiO2 nanowire arrays for photoelectrochemical water splitting.** *Nano Lett* 2011, **11:**3026–3033.
27. Yan J, Khoo E, Sumboja A, Lee PS: **Facile coating of manganese oxide on Tin oxide nanowires with high-performance capacitive behavior.** *ACS Nano* 2010, **4:**4247.
28. Dong SM, Chen X, Gu L, Zhou XH, Li LF, Liu ZH, Han PX, Xu HX, Yao JH, Wang HB, Zhang XY, Shang CQ, Cui GL, Chen LQ: **One dimensional MnO2/titanium nitride nanotube coaxial arrays for high performance electrochemical capacitive energy storage.** *Energy Environ Sci* 2011, **4:**3502.
29. Lu T, Pan LK, Li HB, Zhu G, Lv T, Liu XJ, Sun Z, Chen T, Daniel HU: **Chua: Microwave-assisted synthesis of graphene-ZnO nanocomposite for electrochemical supercapacitors.** *J Alloys Compd* 2011, **509:**5488–5492.
30. Wu J, Wang ZM, Holmes K, Marega E Jr, Zhou Z, Li H, Mazur YI, Salamo GJ: **Laterally aligned quantum rings: from one-dimensional chains to two-dimensional arrays.** *Applied Physics Letters* 2012, **100:**203117.
31. Lu T, Zhang Y, Li H, Pan L, Li Y, Sun Z: **Electrochemical behaviors of graphene-ZnO and grapheme-SnO_2 composite films for supercapacitors.** *Electrochim Acta* 2010, **55:**4170–4173.
32. Guo G, Huang L, Chang Q, Ji L, Liu Y, Xie Y, Shi W, Jia N: **Flexible and transparent supercapacitor based on In2O3 nanowire/carbon nanotube heterogeneous films.** *Appl Phys Lett* 2011, **99:**83111–83113.
33. Zhang YP, Li HB, Pan LK, Lu T, Sun Z: **Capacitive behavior of graphene-ZnO composite film for supercapacitors.** *J Electroanal Chem* 2009, **634:**68–71.
34. Wang J, Gao Z, Li Z, Wang B, Yan Y, Liu Q, Mann T, Zhang M, Jiang Z: **Green synthesis of graphene nanosheets/ZnO composites and electrochemical properties.** *J Solid State Chem* 2011, **184:**1421–1427.
35. Lu T, Pan L, Li H, Zhu G, Lv T, Liu X, Sun Z, Chen T, Chua DHC: **Microwave-assisted synthesis of graphene–ZnO nanocomposite for electrochemical supercapacitors.** *J Alloys Compd* 2011, **509:**5488–5492.
36. Qin Z, Li ZJ, Zhang M, Yang BC, Outlaw RA: **Sn nanoparticles grown on graphene for enhanced electrochemical properties.** *J Power Sources* 2012, **217:**303–308.
37. Dubal DP, Holze R: **All-solid-state flexible thin film supercapacitor based on Mn3O4 stacked nanosheets with gel electrolyte.** *Energy* 2013, **51:**407e412.
38. Kim YJ, Lee JH, Yi GC: **Electrochemical growth of vertically aligned ZnO nanorod arrays on oxidized bi-layer graphene electrode.** *Appl Phys Lett* 2009, **95:**213101.
39. Kim SR, Parvez MK, Chhowalla M: **UV-reduction of graphene oxide and its application as an interfacial layer to reduce the back-transport reactions in dye-sensitized solar cells.** *Chem Phys Lett* 2009, **483:**124.
40. Chen J, Li C, Eda GK, Zhang Y, Lei W, Chhowalla M, Milne WI, Deng WQ: **Incorporation of graphene in quantum dot sensitized solar cells based on ZnO nanorods.** *Chem Commun* 2011, **47:**6084–6086.
41. Alim KA, Fonoberov VA, Shamsa M, Balandin AA: **Micro-Raman investigation of optical phonons in ZnO nanocrystals.** *J Appl Phys* 2005, **97:**124313–124317.
42. Li ZP, Mi YJ, Liu XH, Liu S, Yang SR, Wang JQ: **Flexible graphene/MnO_2 composite papers for supercapacitor electrodes.** *J Mater Chem* 2011, **21:**14706–14711.
43. Kang YJ, Chung H, Han CH, Kim W: **All-solid-state flexible supercapacitors based on papers coated with carbon nanotubes and ionic-liquid-based gel electrolytes.** *Nanotechnology* 2012, **23:**065401.
44. Jayalakshmi M, Palaniappa M, Balasubramanian K: **Combustion synthesis of ZnO/carbon composite and its electrochemical characterization for supercapacitor application.** *Int J Electrochem Sci* 2008, **3:**96–103.

doi:10.1186/1556-276X-8-473
Cite this article as: Li *et al.*: High-performance solid-state supercapacitors based on graphene-ZnO hybrid nanocomposites. *Nanoscale Research Letters* 2013 **8**:473.